Reversible Electrochemical Switching of Polymer Brushes Grafted onto Conducting Polymer Films

ARTICLE *in* LANGMUIR · MAY 2012

Impact Factor: 4.46 · DOI: 10.1021/la301031b · Source: PubMed

3 AUTHORS:

Yiwen Pei
Curtin University
19 PUBLICATIONS **153** CITATIONS
SEE PROFILE

Jadranka Travas-Sejdic
University of Auckland
199 PUBLICATIONS **3,476** CITATIONS
SEE PROFILE

David E Williams
University of Auckland
338 PUBLICATIONS **7,495** CITATIONS
SEE PROFILE

Langmuir

Article

pubs.acs.org/Langmuir

Reversible Electrochemical Switching of Polymer Brushes Grafted onto Conducting Polymer Films

Yiwen Pei,[†] Jadranka Travas-Sejdic,[†,‡] and David E. Williams*[,†,‡]

[†]Polymer Electronic Research Centre, School of Chemical Sciences, University of Auckland, Private Bag 92019, Auckland 1142, New Zealand

[‡]MacDiarmid Institute for Advanced Materials and Nanotechnology, Wellington, New Zealand

Supporting Information

ABSTRACT: We demonstrate the electrochemical switching of conformation of surface-bound polymer brushes, by grafting environmentally sensitive polymer brushes from an electrochemically active conducting polymer (ECP). Using atom transfer radical polymerization (ATRP), we grafted zwitterionic betaine homopolymer and block copolymer brushes of poly(3-(methacryloylamido)propyl)-*N*,*N*′-dimethyl(3-sulfopropyl)-ammonium hydroxide) (PMPDSAH) and poly(methyl methacrylate)-*b*-PMPDSAH, from an initiator, surface-coupled to a poly(pyrrole-*co*-pyrrolyl butyric acid) film. The changes in ionic solution composition in the surface layer, resulting from oxidation and reduction of the ECP, trigger a switch in conformation of the surface-bound polymer brushes, demonstrated here by electrochemical impedance spectroscopy (EIS) and in a change of wettability. The switch is dependent upon temperature in a way that is analogous to the temperature-dependent solubility and aggregation of similar betaine polymers in aqueous solution but has a quite different dependence on salt concentration in solution. The switch is fully reversible and reproducible. We interpret the switching behavior in terms of a transition to a "supercollapsed" state on the surface that is controlled by ions that balance the charge state of the ECP and are adsorbed to the opposite charges of the zwitterionic graft, close to the graft−ECP interface. The behavior is significantly modified by hydrophobic interactions of the block copolymer graft. We speculate that the synergistic combination of properties embodied in these "smart" materials may find applications in electrochemical control of surface wetting and in the interaction with biomolecules and living cells.

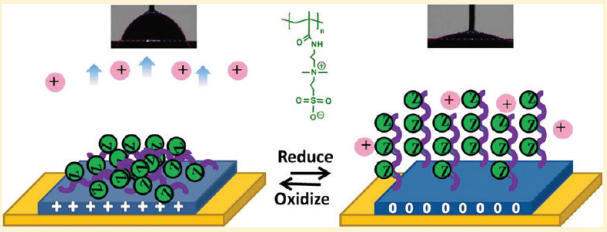

1. INTRODUCTION

The present work was stimulated by the studies of Huck et al. on the change of properties caused by changes of the conformation of a surface-bound polyelectrolyte brush, caused either by a change of temperature or of solution composition.[1−8] These authors have recently demonstrated the electrochemically driven actuation of microcantilevers, where a reversible perturbation of the electrical double layer causes ion transport into and out of a grafted polymer brush, resulting in conformational changes of the grafted polymer layer.[9] Electrochemically active conducting polymers (ECPs)[10−13] have an interesting property of ion exchange driven by a redox process that is also coupled to changes in electrical conductivity, optical properties, and volume. The properties can be modulated by the choice of ionic dopant and by the choice of exchangeable ion. Thus, we have explored the idea that the ion flux associated with the redox reaction of an ECP could cause a change of conformation of a suitably formulated polymer that was grafted from the surface. Out of this comes a new method for electrochemical control of surface wettability or adhesion. Controlling wetting properties of a surface is significant in many applications, such as microfluidic devices, low friction surfaces, and thin film sensors.[14−17] By suitably altering the surface energy of "smart" materials, wettability gradients can be set up and used to induce fluid movements. Recently, ECP doped with surfactant anions have been shown to switch wetting state by an electric stimulus.[12,14,15,17−20]

Surface-initiated growth of polymer brushes has been extensively investigated. The resultant properties of course depend upon the surface density of the brush and upon its chemical nature.[21,22] Atom transfer radical polymerization (ATRP) is an elegant and efficient method to produce a polymer with well-controlled molecular weight and low polydispersity[23] and is well-adapted for surface grafting using a surface-attached initiator. The "grafting from" technique provides control over the density of polymer chains on a surface.[24] The possibility of using a surface-initiated polymerization to graft another polymer from the surface of an ECP has been demonstrated: Roux et al.[25] employed a surface initiated polymerization to grow polystyrene from a carboxylic acid functionalized polypyrrole surface, and Strover et al. have recently described grafting of polystyrene-*b*-poly(acrylic acid) from a poly(terthiophene).[26]

Received: March 10, 2012
Revised: April 30, 2012
Published: May 2, 2012

dx.doi.org/10.1021/la301031b | *Langmuir* 2012, 28, 8072−8083

Scheme 1. Synthesis of PMPDSAH-Grafted (1) and PMMA-*b*-PMPDSAH-Grafted (2) Poly(Py-*co*-PBA) Films[a]

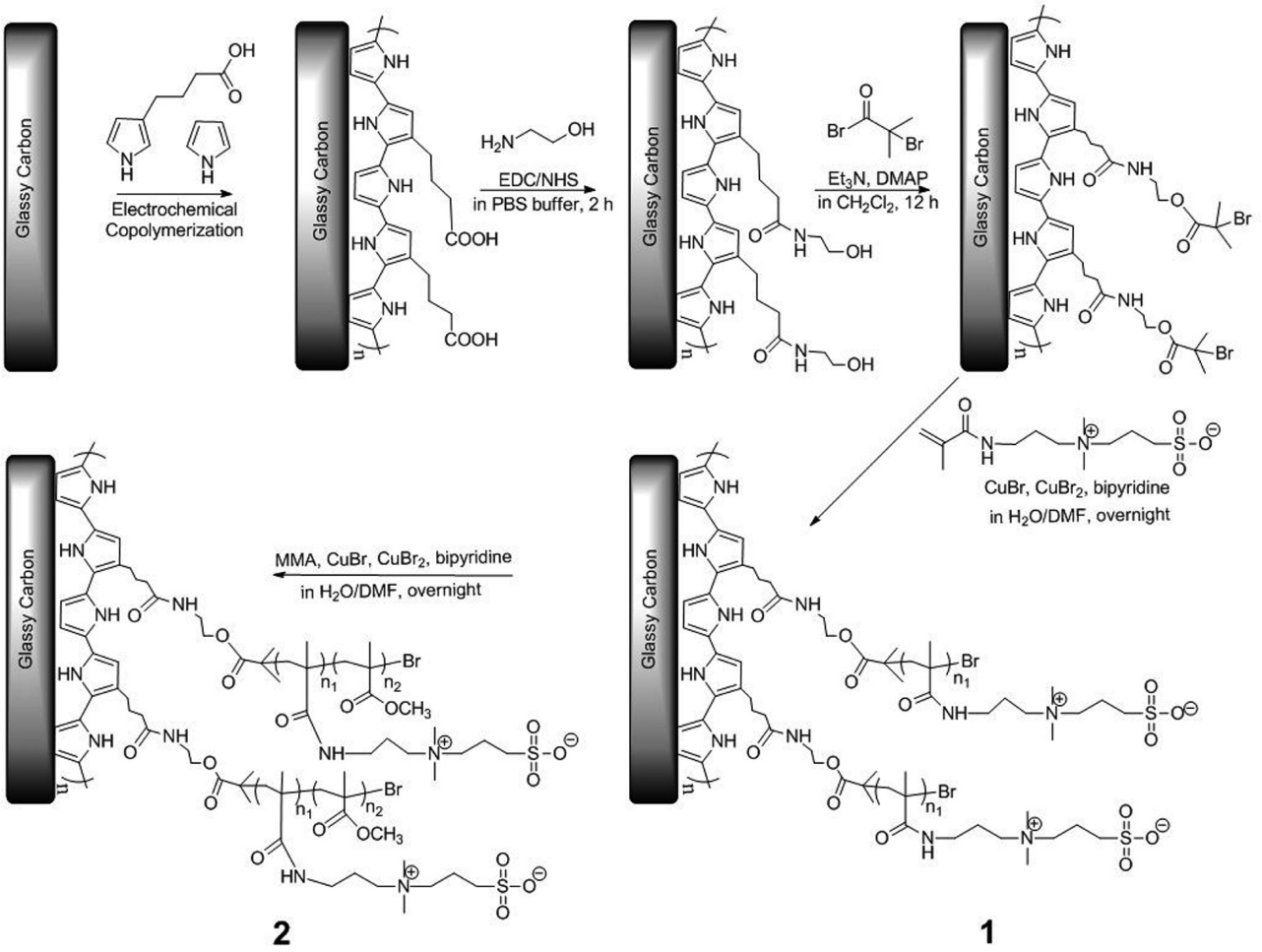

[a]Abbreviations: phosphate-buffered saline, PBS; 1-ethyl-3-(3-dimethylaminopropyl)carbodiimide, EDC; *N*-hydroxysuccinimide, NHS; triethylamine, Et_3N; 4-(dimethylamino)pyridine, DMAP; dimethyl formamide, DMF; 2,2′-bipyridyl, Bipy; methyl methacrylate, MMA.

Zwitterionic polymeric betaines, such as poly(3-(methacryloylamido)propyl)-*N*,*N*′-dimethyl(3-sulfopropyl)-ammonium hydroxide) (PMPDSAH), have extremely high dipole moment leading to a range of unique properties as a consequence of strong inter- and intramolecular interactions.[27] They show an upper critical solution temperature (UCST) that must be exceeded for transition from water-insoluble to water-soluble, which is significantly decreased upon addition of salts: the so-called "anti-polyelectrolyte" effect.[28−31] The important effects are directed dipole−dipole interactions between the zwitterionic side chains of the polymer, which promote the formation of organized molecular aggregates that are broken up by an osmotic pressure effect upon addition of salt.[32] The effects are significantly modified by an asymmetry in adsorption of the ions of the electrolyte onto the anionic and cationic sites of the polymer.[31,33] The solution properties of these polymers are modified in interesting ways when hydrophobic elements are introduced, depending upon the balance between dipolar (zwitterionic) and hydrophobic interactions.[34] Random co-polymers of acrylamide and acryloylsulfobetaine showed extreme sensitivity of solution conformation to change of solution pH or salt concentration.[35] Lower concentrations of salt caused disaggregation, but higher concentrations caused an enhancement of aggregation.[36]

The possibility of surface modification of a solid substrate using thermoresponsive and salt-responsive zwitterionic polymers has stimulated intensive research interest[37] and found applications in designing biocompatible surfaces,[38−40] enhancing efficiency of antibiofouling coating,[41] transferring proteins,[42] and controlling electro-osmotic flow in microfluidics.[43] Recently, it has been reported that poly(zwitterions) conjugated to proteins can significantly increase the stability and improve the binding affinity or bioactivity of the protein.[44] Collapse and expansion of poly(zwitterionic) brushes grafted onto polymer[45] or silica[46] particles, driven by the change of temperature[45] or salt concentration in solution,[46] has been demonstrated recently.

Here, we report the synthesis of PMPDSAH-grafted and PMMA-*b*-PMPDSAH-grafted poly(pyrrole-*co*-pyrrolyl butyric acid) [poly(Py-*co*-PBA)] films via ATRP (MMA, methyl methacrylate). The resulting films were characterized by scanning electron microscopy (SEM), X-ray photoelectron spectroscopy (XPS), cyclic voltammetry (CV), electrochemical impedance spectroscopy (EIS), and contact angle measurement. EIS has proven to be an extremely powerful method for following in situ the conformational changes of such grafted layers.[5] We have demonstrated electrochemically controlled conformational changes of the grafted films driven by the oxidation and reduction of the conducting polymer. Moreover,

dx.doi.org/10.1021/la301031b | *Langmuir* 2012, 28, 8072−8083

these changes have been shown to be sensitive to change of temperature and salt concentration in solution.

2. EXPERIMENTAL SECTION

2.1. Materials. All reagents were purchased from Sigma-Aldrich and used as received. Pyrrole was distilled under reduced pressure and kept in N_2 atmosphere at 0 °C. MMA was washed twice against aqueous 5% (w/v) sodium hydroxide, to remove the inhibitor, and distilled under vacuum just before use.

2.2. Synthesis of Poly(Py-*co*-PBA) on Glassy Carbon Electrodes. Electrochemical copolymerization was performed at room temperature using a CH Instrument potentiostat (model 650). A three-electrode system comprised a glassy carbon working electrode (4 mm × 25 mm × 2.5 mm) masked using Kapton tape to expose an area of 0.6 cm^2 (4 mm × 15 mm), a Ag/AgCl (3 M KCl) reference electrode, and a Pt wire counter electrode. Poly(pyrrole-*co*-pyrrolyl butyric acid) films were electrochemically synthesized in a solution of 0.5 M pyrrole (Py), 0.1 M 4-(3-pyrrolyl) butyric acid (PBA), 0.2 M LiCl, and 0.57 M H_2SO_4 in methanol by applying a fixed potential of 0.75 V (vs Ag/AgCl, 3 M KCl). Film thickness was estimated to be 3 μm by controlling total charge passed (0.36 C) during polymerization.[47] The Kapton tape was removed after polymerization. The resulting films were cycled four times in 0.2 M LiCl methanol solution and four times in 1 mM NaCl(aq) at a scan rate of 0.1 and 0.01 V s^{-1}, over a range from −0.8 to +0.4 V (vs Ag/AgCl, 3 M KCl). The films were rinsed with Milli-Q water between electrolytes. All films were reduced at −0.8 V (vs Ag/AgCl, 3 M KCl) for 3 min in 1 mM NaCl(aq) before further chemical treatment.

2.3. Covalent Attachment of ATRP Initiator on Poly(Py-*co*-PBA). Surface modification involves two steps: converting carboxylate to a reactive hydroxyl group and then attaching the ATRP initiator by a nucleophilic substitution reaction. First, the glassy carbon electrode carrying the poly(Py-*co*-PBA) film was immersed in 5 mL of phosphate-buffered saline (PBS) solution (pH 5.2) containing 0.27 g of 1-ethyl-3-(3-dimethylaminopropyl)carbodiimide (EDC), 0.41 g of *N*-hydroxysuccinimide (NHS), and 53 μL of ethanolamine. The reaction was carried out for 2 h at room temperature and then the film was washed with Milli-Q water and then dichloromethane (CH_2Cl_2). Second, for the attachment of the ATRP initiator, a solution of 23 μL of triethylamine and 0.01 g of 4-(dimethylamino)pyridine in 2 mL of anhydrous dichloromethane was added into a small vial containing a modified poly(Py-*co*-PBA) film on a glassy carbon electrode. The vial was then sealed and kept at 0 °C for 10 min while 17 μL of α-bromoisobutyryl bromide was slowly added. The reaction mixture was kept at room temperature for 12 h. The resulting surface was washed with Milli-Q water, dimethylformamide (DMF), and CH_2Cl_2. We followed this procedure to ensure attachment of the ATRP initiator because the common reaction of acylation at the 2-position is excluded, since this is the site of polymerization of pyrrole. There is indeed also the possibility of N-acylation, but this reaction is reported to be slow at room temperature.[48]

2.4. Grafting PMPDSAH, PMMA-*b*-PMPDSAH with Poly(Py-*co*-PBA) via ATRP. All radical polymerizations were conducted in Schlenk tubes at room temperature under N_2 atmosphere. Preparation of a PMPDSAH-grafted poly(Py-*co*-PBA) film proceeded as follows. A surface-modified poly(Py-*co*-PBA) film on a glassy carbon electrode was placed into a 50 mL Schlenk tube and the whole tube was degassed for 20 min. A solution containing 2 g of MPDSAH, 0.16 g of 2,2′-bipyridyl, 0.07 g of CuBr, and 0.01 g of $CuBr_2$ in 20 mL of water/DMF mixture (4:6, v/v) was degassed by three freeze−pump−thaw cycles and carefully injected into the Schlenk tube via a syringe. Then, the tube was sealed and the reaction mixture was slowly stirred at room temperature overnight, taking care not to touch the films. After the polymerization, the resulting film was rinsed with DMF and Milli-Q water. For block copolymerization, a solution of 0.5 g of MMA, 0.16 g of 2,2′-bipyridyl, 0.07 g of CuBr, and 0.01 g of $CuBr_2$ in 20 mL of water/DMF mixture (4:6, vol/vol) was degassed and injected into the Schlenk tube containing a glassy-carbon-supported PMPDSAH-grafted poly(Py-*co*-PBA) film. The reaction mixture was slowly stirred overnight under N_2 atmosphere. After the reaction, the surfaces were rinsed with warm Milli-Q water (60 °C) and dried under a stream of N_2 (see Scheme 1)

2.5. Characterizations. *2.5.1. SEM, XPS, and FTIR Measurements.* The morphology of all the films was studied using scanning electron microscopy (SEM) (Philips XL30S FEG without sputter coating with metal). X-ray photoelectron spectroscopy (XPS) measurements were made using a Kratos Axis Ultra spectrometer with an Al Kα source (1486.7 eV). The X-ray source was run at a reduced power of 150 W. The pressure in the analysis chamber was maintained at 10^{-10} Torr during the measurements. Data were analyzed using the CasaXPS software program. Core level scans were calibrated for the neutralizer shift using the C 1s signal from saturated hydrocarbon at 285.0 eV. Core level data were fitted using Gaussian−Lorentzian peaks with a Shirley background. The peak full width at half-maximum (fwhm) was maintained constant for all the components in a particular spectrum. Fourier transform infrared spectroscopy (FTIR) measurements were performed by a Continuum FTIR microscope equipped with a liquid nitrogen cooled MCT detector in reflectance mode with aperture size 100 μm × 100 μm with Atlμs spectroscopic software.

2.5.2. Electrochemical Measurements. A conventional three-electrode cell (6 mL) with a modified glassy carbon working electrode (without Kapton tape masking), a Pt wire counter electrode, and an Ag/AgCl (3 M KCl) reference electrode was employed for electrochemical characterization. Cyclic voltammetry was measured at room temperature using a CH Instrument potentiostat (model 650). The electrolyte was an aqueous solution of sodium chloride, with concentration increased stepwise from lowest to highest, with scan rate decreased from highest to lowest in each electrolyte. All cycles started with the film in the reduced state, at −0.8 V (vs Ag/AgCl, 3 M KCl). Impedance measurements were conducted using an EG&G potentiostat/galvanostat (Princeton Applied Research, model 280) and an EG&G 1025 frequency response analyzer. Impedance measurements were performed with 5 mV sinusoidal modulation amplitude at an applied bias potential of +0.4 or −0.8 V (vs Ag/AgCl, 3 M KCl). The impedance data were measured from 10 kHz to 0.1 Hz at 10 points per decade. The series resistance due to the electrolyte solution, R_s, was determined from an impedance diagram, by extrapolation of the high-frequency data to the real impedance axis.

2.5.3. Equivalent Circuit Fitting. The porous polymer film is best represented as a transmission line. This equivalent circuit model has been extensively developed by Bisquert et al.[49−52]

Here we present a simplified version of Bisquert's model that can sufficiently describe the main features of the impedance data. The transmission line is described by a characteristic length. If this is much greater than the film thickness, then the system behaves as a uniformly accessible surface with impedance described by the polymer-solution interface impedance averaged over the thickness of the layer, with the resistances due to the electrolyte and polymer phases being absorbed into a simple series resistance, R_s. As shown in Figure 1, the simplified impedance model involves a distributed constant-phase element (CPE) with fractional exponent $0 < \alpha_1 < 1$ and prefactor q_1, in parallel with a resistive element R_1, which is in series with another CPE ($0 < \alpha_2 < 1$). The impedance of this circuit is given by the following equation (ω denotes the angular frequency):

$$Z = R_s + \left[q_1(i\omega)^{\alpha_1} + \left(\frac{1}{q_2(i\omega)^{\alpha_2}} + R_1 \right)^{-1} \right]^{-1} \quad (1)$$

These circuit elements can be interpreted as a double layer capacitance associated with the conducting polymer film−solution interface (q_1) and a type of surface-state capacitance (q_2) that is charged through the conducting polymer or by ionic diffusion in the polymer brush layer characterized by resistance R_1. In our experimental configuration, since the glassy carbon support was not masked, the element q_1 also has a fixed parallel contribution due to the part of the carbon surface that was not coated with conducting polymer. Moreover, we assume that the deviation from nonideality captured in the exponents α_1 and α_2 is largely due to the surface

dx.doi.org/10.1021/la301031b | *Langmuir* 2012, 28, 8072−8083

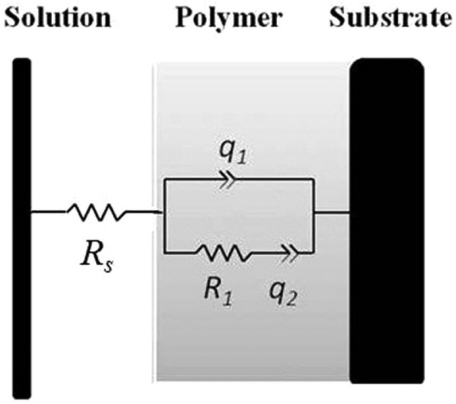

Figure 1. Simplified model for a thin porous conducting polymer film, following Bisquert et al.,[49,52] used for fitting and interpretation of the impedance data.

roughness, which we assume affects both constant phase elements in the same way, so we set $\alpha_1 = \alpha_2 = \alpha$ to minimize the number of variable parameters for the fitting. The impedance spectrum was fitted using the nonlinear least-squares algorithm Solver in an Excel spreadsheet. Two methods for estimation of errors in the fitted parameters were used.[53−55] The macro SolverAid[56] provided parameter uncertainty estimates based on the partial derivatives. Also, normally distributed errors with standard deviation (1%) determined from repeated measurement of a model circuit were added to the experimental data, and the results were refitted; estimated errors in the fitted parameters were obtained from the results of ten such trials. We confirmed that the full transmission line model[52] did not yield an improvement in fitting of the data sufficient to justify the additional parameters (with associated uncertainty) that were required.

2.5.4. Contact Angle Measurement. In situ electrochemical switching of surface energy of PMPDSAH-grafted and unmodified poly(Py-*co*-PBA) films was studied using a contact angle meter (CAM 100, KSV instrument) and an electrochemical workstation (model 650, CH Instruments). A two-electrode system comprised a polymer-coated glassy carbon electrode and a Pt wire. A droplet of 5 μL of 0.001 M NaCl(aq) electrolyte was applied on a polymer-coated glassy carbon electrode, and a fine Pt wire was then immersed into the droplet, taking care not to touch the surface. The films were first oxidized at a cell potential difference of +0.4 V for 180 s and then reduced at a cell potential difference of −0.8 V for 540 s. Mean contact angles of both films were recorded every 180 s.

3. RESULTS

3.1. Structure of Polymer Films. All conducting polymer films were obtained electrochemically at a fixed potential of 0.75 V (vs Ag/AgCl, 3 M KCl). The resulting film thickness was controlled by the amount of total charge supplied (0.36 C) by the electrode, and the film thickness (≈3 μm) was estimated using literature parameters.[47] A variety of polymer brushes were grafted from the modified poly(Py-*co*-PBA) films by ATRP. Figure 2 shows intact microstructures of the modified films after chemical reactions, as compared with that of the unmodified film. The films were, however, fragile and could become detached from the glassy carbon support. The presence of the grafted polymer layer was confirmed by XPS (Figure 3) and FTIR.

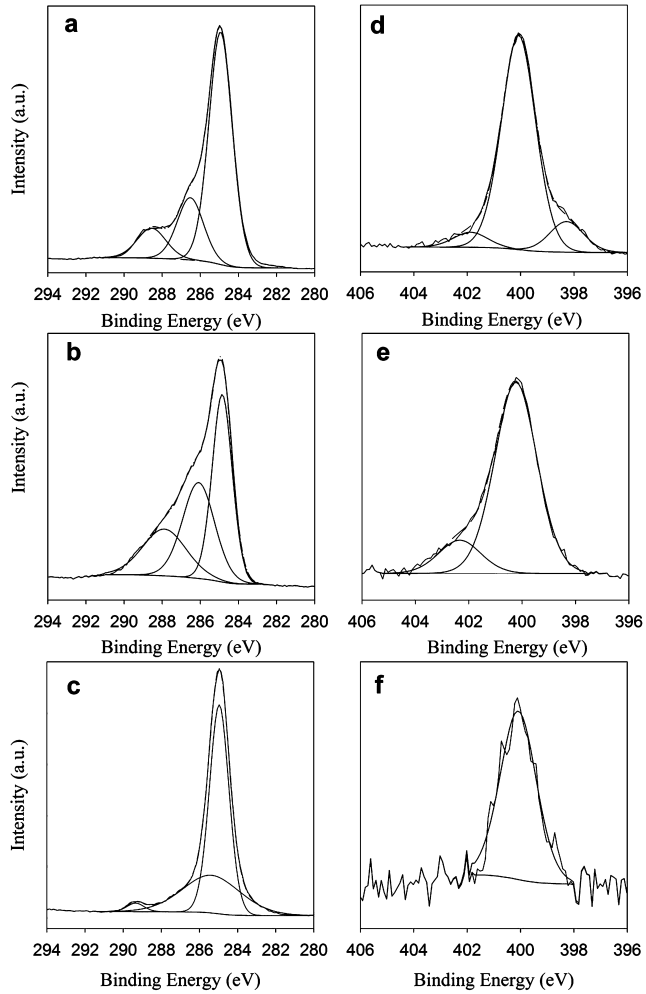

Figure 3. C 1s core level spectra (a−c) and N 1s core level spectra (d−f) of unmodified (a, d) and PMPDSAH-grafted (b, e) and PMMA-*b*-PMPDSAH-grafted (c, f) poly(Py-*co*-PBA) films.

The XPS C 1s core level spectra for the unmodified, PMPDSAH-grafted and PMMA-*b*-PMPDSAH-grafted poly(Py-*co*-PBA) films are shown in Figure 3a−c. Broad and asymmetric

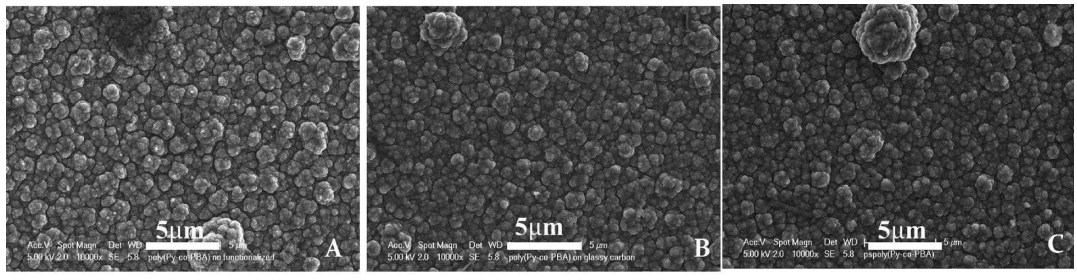

Figure 2. SEM images of (A) the unmodified, (B) PMPDSAH-grafted, and (C) PMMA-*b*-PMPDSAH-grafted poly(Py-*co*-PBA) films.

dx.doi.org/10.1021/la301031b | *Langmuir* 2012, 28, 8072−8083

peaks of all samples were decomposed into three subbands, centered at 284.9, 286.9, and 288.5 eV, respectively, which varied in relative intensity and peak width and slightly in peak position with increasing functionalization of the surface. Figure 3d–f shows the XPS N 1s core level spectra for the modified and unmodified films. For the unmodified film, the main peak was centered at 400.1 eV with two shoulders at 398.4 and 401.8 eV. For PMPDSAH-grafted poly(Py-*co*-PBA) film, an asymmetric peak was observed that could be decomposed into two subbands, at 400.2 and 402.4 eV. For PMMA-*b*-PMPDSAH-grafted films, only a single peak at 400.2 eV was observed. The presence of the grafted polymer layers, PMPDSAH and PMMA-*b*-PMPDSAH, was further confirmed by observation of a sulfur signal at 170 eV, with estimated concentration 0.18 and 0.10 atom %, which is absent in the unmodified film. A weak bromine signal (72 eV) was observed for the PMPDSAH-grafted layer but not for the PMMA-*b*-PMPDSAH-grafted film. The FTIR spectrum of the PMMA-b-PMPDSAH-grafted layers showed the presence of the OCH_3 symmetric stretch at 1445 cm^{-1} and the α-CH_3 symmetric C–H bending vibration at 1388 cm^{-1}, which were absent in the unmodified film (Supporting Information).

3.2. Cyclic Voltammetry. The electrochemical activity of the modified and unmodified thin film electrodes was examined in aqueous solutions of sodium chloride at 22 °C. Figure 4A–C

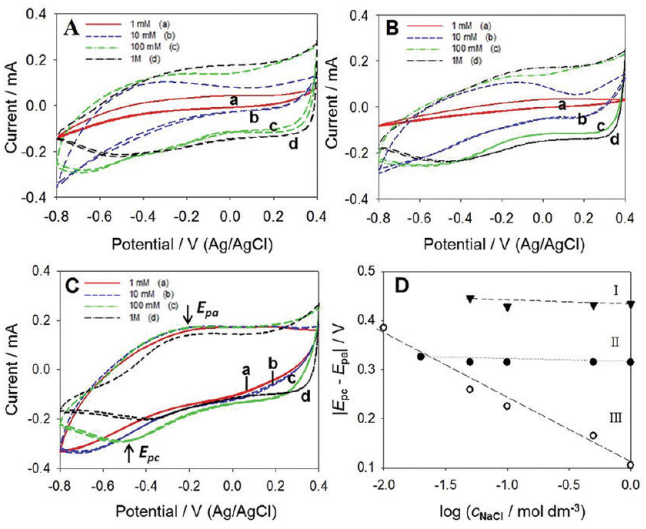

Figure 4. Cyclic voltammograms of (A) the unmodified, (B) PMPDSAH-grafted, and (C) PMMA-*b*-PMPDSAH-grafted poly(Py-*co*-PBA) films in (a) 0.001 M, (b) 0.01 M, (c) 0.1 M, and (d) 1 M NaCl(aq). Scan rate is 0.01 V s^{-1}. (D) The difference between anodic and cathodic peak potential (vs Ag/AgCl, 3 M KCl) of (I) the unmodified, (II) PMPDSAH-grafted, and (III) PMMA-*b*-PMPDSAH-grafted poly(Py-*co*-PBA) films as a function of salt concentration at 22 °C. This temperature is below the transition temperature in 0.01 M NaCl(aq) for the PMMA-*b*-PMPDSAH film and above that for the PMPDSAH film (see section 3.3.2).

show the cyclic voltammograms of the obtained films in various concentrations of the electrolyte (0.001, 0.01, 0.1, and 1 M) at a scan rate of 0.01 V s^{-1}. The broad voltammetric envelope characteristic of conducting polymers was observed for each of the three types of polymer film, with subtle but clear differences in behavior according to the modification. Though broad, the waves could be characterized by an anodic and cathodic peak potential. The shape (both magnitude and peak position) of the voltammograms varied with the salt concentration, differently for the unmodified poly(Py-*co*-PBA) films and for the brush-grafted films. The waves opened out with increasing salt concentration in the electrolyte, with the cathodic peak moving to more positive potentials: this effect was rather less marked for the PMPDSAH-grafted film than for PMMA-*b*-PMPDSAH-grafted film. The anodic peak stayed at approximately constant potential for both the grafted films, but moved to more positive potential for the unmodified film, with increasing salt concentration. Figure 4D shows the effect of salt concentration on the separation of oxidation and reduction peak potentials ($E_{pa} - E_{pc}$, symbolized by ΔE_p) for all the films. The peak separation for unmodified and PMPDSAH-grafted films was not influenced by the addition of salt. However, ΔE_p for the PMMA-*b*-PMPDSAH grafts changed from 0.4 to 0.1 V as salt concentration increased.

3.3. EIS Study of Polymer Conformation Change. *3.3.1. Effect of Electrode Potential at a Fixed Temperature.* Impedance measurements were conducted at a fixed potential of +0.4 V (fully oxidized state) or −0.8 V (fully reduced state) (Figure 4). The main concern in this study is the capacitance behavior of the charged/uncharged polymer films. Cole–Cole diagrams (capacitance plots) were generated by subtracting the series resistance R_s from the impedance, $C(\omega)_{corr} = 1/i\omega[Z(\omega) - R_s]$. Examples of capacitance plots in the reduced state (E = −0.8 V) and in the oxidized state (E = +0.4 V) of various films in 0.5 M NaCl(aq) solution (18 °C) are given in Figure 5. In the reduced state, the capacitance plots were very similar for all the films, modified and unmodified. In the oxidized state, however, a very significant diminution of capacitance of the modified films compared to the unmodified ones was observed.

3.3.2. Effect of Temperature. The effect of temperature on the capacitance of PMPDSAH- and PMMA-*b*-PMPDSAH-grafted films was followed by successive impedance measurements in 0.01 M $NaCl_{aq}$ applying a potential of +0.4 V or −0.8 V (vs Ag/AgCl, 3 M KCl). Films were first reduced and then oxidized at each temperature. As shown in Figure 6, the capacitance in the oxidized state of the PMPDSAH-grafted film changed dramatically over the small temperature range from 18 to 23 °C, such that at the higher temperature the behavior had become qualitatively similar to that of the unmodified film. The capacitance in the reduced state was hardly affected. A similar effect was observed for the PMMA-*b*-PMPDSAH-grafted film (Figure 7) though over a different temperature range. A large difference of the capacitance plots between the oxidized and reduced polymer was observed at 15 °C; the difference between the two states was less at 23 °C and had essentially disappeared at 35 °C.

3.3.3. Effect of Salt Concentration. In all the experiments described in this section, the electrochemical state was switched from oxidized to reduced and then back to oxidized, after which the salt concentration in solution was incremented, starting from the most dilute. The consistency of the derived parameters strongly implies that the consequent switch of surface state of the graft was repeatable and reversible. We further checked by remeasuring samples in a low salt concentration after the sequence of measurements up to high salt concentration and confirmed that we could recover the originally measured state.

As illustrated in Figure 5, the circuit of Figure 1 represented the data well, except at the highest measurement frequencies, when in some cases an additional series R–q element in parallel with q_2 was needed to fit this part of the data accurately. In the

dx.doi.org/10.1021/la301031b | *Langmuir* 2012, 28, 8072–8083

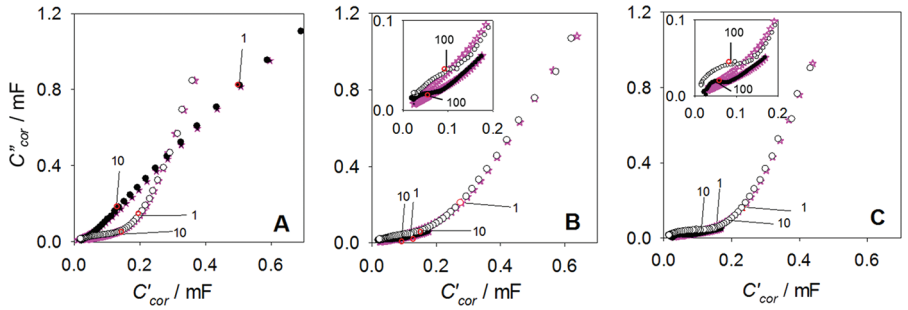

Figure 5. Capacitance plots of (A) the unmodified, (B) PMPDSAH-grafted, and (C) PMMA-*b*-PMPDSAH-grafted poly(Py-*co*-PBA) films in 0.5 M NaCl(aq) solution under an applied potential of (●) +0.4 V or (○) −0.8 V (vs Ag/AgCl, 3 M KCl) at 18 °C. Fitting results for the proposed model are marked (magenta star); labels are frequency in Hz.

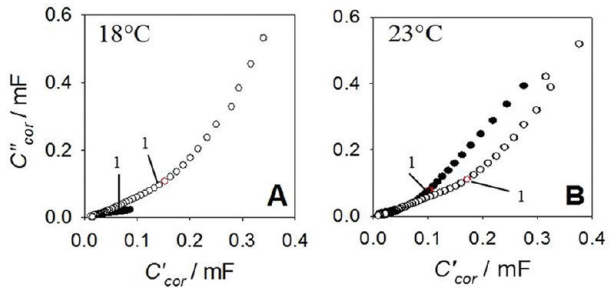

Figure 6. Capacitance plots of PMPDSAH-grafted poly(Py-*co*-PBA) film in 0.01 M NaCl(aq) under an applied potential of (●) +0.4 V or (○) −0.8 V (vs Ag/AgCl, 3 M KCl) at (A) 18 °C and (B) 23 °C.

following, we present the variation of the fitted parameters R_1, q_1, and q_2, in the oxidized and reduced states of the conducting polymer, as a function of salt concentration at a temperature below the transition temperature described above, where the capacitance diagrams for the grafted films showed a strong dependence on the state of oxidation. Except where otherwise mentioned, the parameter uncertainty estimates based on the partial derivatives were less than ±1%, while those based on the Monte Carlo assessment were in the range ±5−10%.

Charging Resistance R_1. Figure 8 illustrates the dependence on salt concentration of the resistance R_1 for the various polymer films. The fitting error in this parameter, as indicated above, was acceptably small for resistances on the scale of 10^5 Ω and lower. For resistances above 10^6 Ω, the quality of the fit was essentially independent of the exact value; hence, these are shown on the diagram just as $>10^6$ Ω. As shown in Figure 8A, the resistance R_1 for the unmodified film did not much vary with the salt concentration in the reduced state and fell steadily with increasing salt concentration in the oxidized state. The resistance values in the oxidized state were lower than in the reduced state. Figure 8B,C shows that the variation of the resistance R_1 for the grafted films was in the reduced state, essentially the same as that of the unmodified film. However, in the oxidized state for the PMPDSAH-grafted film, R_1 showed much larger values in the oxidized state than in the reduced state. Furthermore, there was a sharp decline of R_1 when salt concentration exceeded 0.01 M. The behavior of the PMMA-*b*-PMPDSAH-grafted film was again different: at low salt concentration, in the oxidized state R_1 was similar to that in the reduced state but then increased steadily with salt concentration increasing above 0.01 M.

Surface State Capacitance-like Element q_2. Figure 9A shows that the surface state capacitance-like element q_2 for the unmodified film essentially did not vary, with either the ionic strength or with the oxidation state of the conducting polymer. Figure 9B,C illustrates that, in contrast, the surface state capacitance-like element q_2 of the modified polymer films was very different in the oxidized and reduced states of the conducting polymer and varied differently in response to salt concentration for the zwitterionic homopolymer and for the block copolymer graft. In the oxidized state, q_2 of the PMPDSAH-grafted film had a very large value, regardless of the concentration of NaCl ($q_2 > 1$ F m^{-1} s$^{\alpha-1}$); with such large values, the fit is insensitive to the exact value of q_2. In contrast, as shown in Figure 9C, q_2 of the PMMA-*b*-PMPDSAH-grafted film in the oxidized state was very similar to that in the reduced state at low salt concentration but then abruptly increased to a large value when the salt concentration was increased above 0.01 M.

Fractional Exponent α and Double-Layer Capacitive-like Element q_1. Figure 10 illustrates the fractional exponent α and a double-layer capacitive-like element q_1 for all the polymer

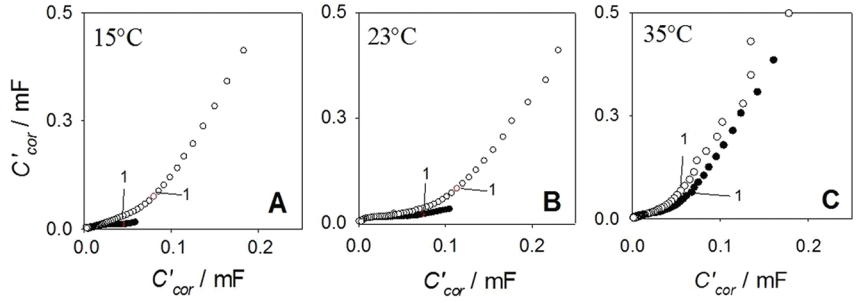

Figure 7. Capacitance plots of PMMA-*b*-PMPDSAH-grafted poly(Py-*co*-PBA) film in 0.01 M NaCl(aq) under an applied potential of (●) +0.4 V or (○) −0.8 V (vs Ag/AgCl, 3 M KCl) at (A) 15 °C, (B) 23 °C, and (C) 35 °C.

dx.doi.org/10.1021/la301031b | *Langmuir* 2012, 28, 8072−8083

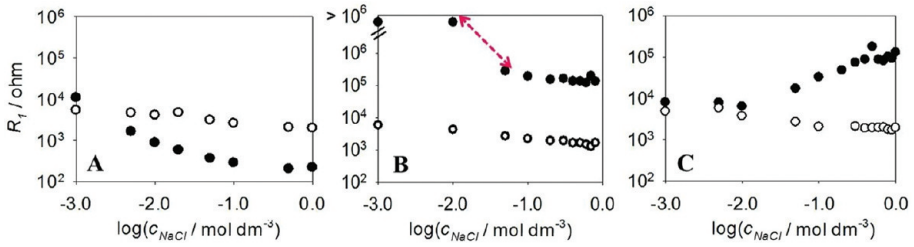

Figure 8. Charging resistance R_1 of (A) the unmodified film, (B) PMPDSAH-grafted, and (C) PMMA-*b*-PMPDSAH-grafted poly(Py-*co*-PBA) films in the oxidized (●) and the reduced state (○), as a function of salt concentration at 18 °C. The estimated standard deviation of the fitted parameters was <10%, except for very large values of R_1, when the fit was essentially insensitive to the exact value.

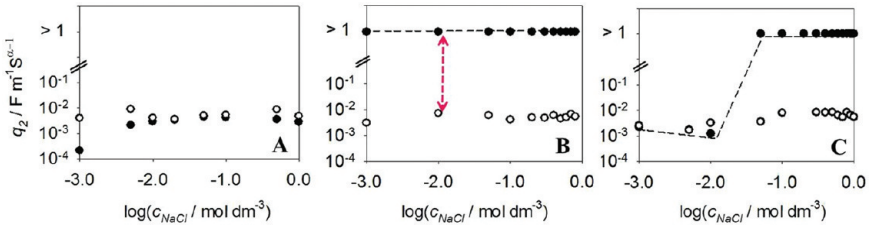

Figure 9. Interfacial capacitance q_2 of (A) the unmodified film, (B) PMPDSAH-grafted, and (C) PMMA-*b*-PMPDSAH-grafted poly(Py-*co*-PBA) films at the oxidized (●) and reduced state (○), as a function of salt concentration at 18 °C. Estimated standard deviation of the fitted parameters was <10%, except for very large values of q_2, for which the fit was essentially insensitive to the exact value.

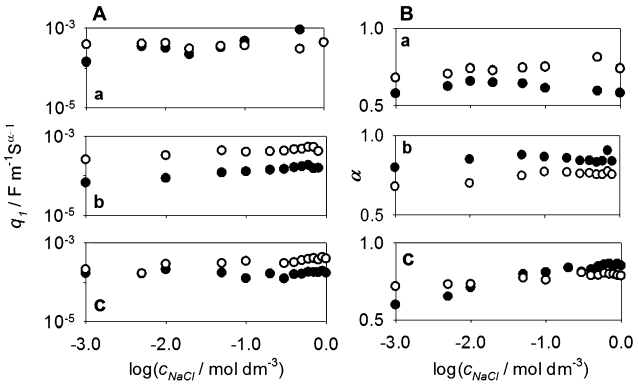

Figure 10. (A) Double-layer capacitance q_1 and (B) fractional exponent α of (a) the unmodified, (b) PMPDSAH-grafted, and (c) PMMA-*b*-PMPDSAH-grafted poly(Py-*co*-PBA) films as a function of salt concentration at 18 °C. All films were first fully oxidized (●) and then reduced (○). The estimated standard deviation of the fitted parameters was <10%.

films as a function of salt concentration, in the oxidized and reduced states. As shown in Figure 10A, all films showed fairly constant q_1 in both the oxidized and reduced states. For the unmodified film, q_1 was essentially the same in both states and invariant with salt concentration. For the modified films, q_1 was higher in the oxidized state, significantly so for the PMPDSAH-grafted film. For the block-copolymer-grafted film, the difference in q_1 in the two states was only noticeable for salt concentration greater than 0.01 M. As noted in the experimental part, the glassy carbon support would have introduced a capacitance in parallel with the polymer film that would add to q_1 and so diminish the effects of the grafted film on variations of this parameter.

Figure 10B shows that the exponent, α, of the constant phase elements varies within the range from 0.6 to 0.8. In the reduced state, α was a constant value (0.75) for all salt concentrations for both the modified and unmodified polymer electrodes. However, in the oxidized state, the exponent α for the unmodified film decreased to approximately 0.6, that for the pMPDSAH-grafted film increased, to approximately 0.85, and that for the pMMA-*b*-pMPDSAH-grafted film increased steadily with increasing salt concentration, from ~0.6 at low concentration to ~0.8 at high concentration.

3.4. Electrolyte Solution Contact Angle. Table 1 illustrates the change in surface wettability induced as a consequence of oxidation or reduction of the polymer film. An auxiliary Pt wire electrode is needed to achieve some degree of control of the electrochemical state of the film, but wetting of this wire causes a change in shape of the drop. The films were also rough, so the results are indicative only. They illustrate a switch in surface wettability of the layer grafted with

Table 1. Effect of the Oxidation State on the Interfacial Tension of PMPDSAH-grafted and Unmodified Poly(Py-*co*-PBA) Films[a]

PMPDSAH-grafted poly(Py-co-PBA)			Unmodified poly(Py-co-PBA)	
Time (s) (state)	CA images	CA (°)	CA images	CA (°)
0 (oxidised)	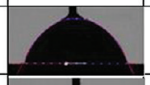	65	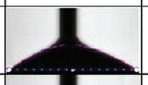	29
180 (end of oxidation)	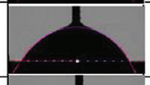	57		23
360 (reduced)	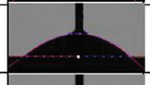	37		20
540 (reduced)	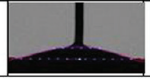	13		21

[a] A 5μL droplet of 1 mM NaCl(aq) was used as the electrolyte. The polymer-coated glassy carbon was the working electrode and fine Pt wire the counter electrode. The films were firstly oxidized at a cell potential difference of +0.4 V for 180 s and then reduced at a cell potential difference of −0.8 V for 540 s.

dx.doi.org/10.1021/la301031b | *Langmuir* 2012, 28, 8072−8083

PMPDSAH. The behavior of the layer grafted with the block copolymer was not measured in this way.

4. DISCUSSION

These results demonstrate that the aim of this work, a reversible electrically controlled switch of surface property of surface-modified conducting polymer films, has been achieved.

SEM images indicate that although the films were fragile, the extensive synthetic manipulations had not destroyed the microstructure of the polymer or resulted in the disintegration of the film. Compelling evidence for successful grafting of (co)polymer brushes is given by XPS, as shown in Figure 3. The C 1s and N 1s core level spectra of all films exhibited broad and asymmetric peaks located at 284.9 and 400.1 eV, which is typical for polypyrrole.[21,57] For the unmodified film, the two subbands at 286.9 and 288.5 eV can be assigned to $-O-CH_2-$[58] and [O−(C═O)],[59] resulting from the carboxyl side chains from pyrrolyl butyric acid. The two shoulders (398.4 and 401.8 eV) are attributed to static disorder effects and electrostatic effects from PPy^+Cl^-.[60] As a surface-sensitive technique, XPS analysis profiles the outer 10 nm of a sample; therefore, the surface-bound polymer brushes are more likely to contribute to the measured peaks. According Figure 3b−e, the increasing peak area at 286.3 and 402.5 eV can be attributed to amide (C−N) and quaternary ammonium (N^+),[61] indicative of the successful grafting of sulfobetaine polymers. For the PMMA-*b*-PMPDSAH-grafted polymer film, the evidence for the surface-grafted PMMA block copolymer is best highlighted by the appearance of a new peak at 289.3 eV, which can be assigned to the carbonyl carbon $O{=}C-O-CH_3$.[62,63] The presence of the PMMA block was confirmed by the observation of the OCH_3 symmetric stretching and the α-CH_3 symmetric C−H bending vibrations, characteristic of the methyl methacrylate block[64] in FTIR spectra, as compared to that of the unmodified film.

According to Figure 4A−C, a pair of oxidation and reduction peaks could be observed when the polymer films were cycled in an aqueous solution of sodium chloride (c_{NaCl} > 0.01 M). The first oxidation peak (−0.3 V, vs Ag/AgCl) and its associated reduction peak (−0.6 V) correspond to the peak usually reported in the oxidation scan of polypyrrole.[65,66] Another pair of redox peaks starting just within the potential window studied may relate to the further oxidation process of polypyrrole films in the presence of small anions.[65] Others have ascribed the peaks around −0.3 to −0.6 V Ag/AgCl to cation exchange and peaks around 0 V to anion exchange, for a chloride-doped film cycled in NaCl.[67] Inzelt et al.[68] interpreted quartz-crystal microbalance (EQCM) studies of polypyrrole films in contact with aqueous solutions containing chloride salts of alkali-metal cations as showing that, for thin (100 nm) films, cation expulsion accompanies oxidation of the polymer, while for thick (620 nm) films, cation expulsion occurs at lower potential and the incorporation of anions dominates at higher positive potentials. Gabrielli et al. again with EQCM, demonstrated anion exchange as the dominant process for 200 nm thick films in NaCl electrolyte.[69] Li et al. studied much thicker films (1−2 μm, similar to those studied in our work)[67] and concluded that full oxidation of these films in aqueous NaCl electrolyte involved about 30% cation expulsion and 70% anion insertion. Since the electrochemical reaction involves ion insertion and ejection, the peak height should indeed be sensitive to the salt concentration. As has been noted many times,[68] the details of the ion exchange accompanying the redox reaction are dependent on the thickness, morphology, and composition of the conducting polymer. In our case the process may be further influenced by the effect of the carboxylate groups incorporated into the polymer. The cyclic voltammetry results at low salt concentration are distorted by the effects of ion migration in the solution; however, the peak shift toward positive potential as salt concentration increases indicates that a cation exchange process has occurred.[70] As shown in Figure 4D, a key difference in cyclic voltammograms is the separation between oxidation and reduction peaks: ΔE_p of PMMA-*b*-PMPDSAH-grafted films decreased with increasing salt concentration, compared with a relatively constant ΔE_p of PMPDSAH-grafted and the unmodified film. There is thus a rather subtle effect of the grafted polymer brush on the kinetics of the ion-exchange process that is coupled to the redox process of a conducting polymer film. The conclusion is supported by ac impedance work, as is discussed below. Since the effects in cyclic voltammetry were subtle, the effect of temperature was not explored in detail with this method. One simple but important fact can be taken from the voltammetry results: that the redox process of the conducting polymer, although modified, could indeed be driven through the grafted layer.

Clear evidence of electrochemically controlled switch of conformation of grafted layers is provided by the changes in the Cole−Cole diagrams when the conducting polymer (ECP) was switched between the oxidized and reduced states. As shown in Figure 5, the capacitance of the unmodified film increased as the polymer was oxidized, whereas the capacitance of PMPDSAH-grafted and PMMA-*b*-PMPDSAH-grafted films dramatically decreased. Another major observation was the temperature effect on the Cole−Cole diagrams of the modified films, as shown in Figures 6 and 7. Changes in capacitance of both modified films upon the oxidation and reduction of the ECP diminished with elevating temperature. The major effects were due to the elements of the equivalent circuit that could be attributed to the charging of a surface state (R_1 and q_2 in Figures 8 and 9). In the reduced state of the ECP, these elements were essentially the same for all the films, but in the oxidized state, they were very different and showed a very different behavior with change of salt concentration, provided the temperature was below a critical temperature. Parallels can be found in the literature on the solution properties of PMPDSAH:[31] changes in intra- and intermolecular association caused by screening of the dipoles on the side chains by ions from the electrolyte and by changes in the interactions with water, specifically, the osmotic effects induced as a consequence of distribution of salt between bulk electrolyte and the polymer.[32] However, while the effects of temperature were observed over a similar range for the surface-bound PMPDSAH to that reported for the solution polymer, the electrochemically induced switch in surface state occurred over the full salt concentration range explored (1 mM−2 M).

For the surface-bound PMPDSAH, three different states can be distinguished: that on the reduced ECP, where the graft does not have a big effect on the observed impedance, and two different states on the oxidized ECP, both characterized by a very large surface-state capacitance and with a switch in surface state charging resistance from a lower to a higher value with salt concentration below 0.1 M. The explanation is a simple one for the PMPDSAH surface-grafted conducting polymer: the factor controlling the impedance of the modified film is the grafted layer of polymer brushes, which controls the access of ions from the solution to the ECP interface. If this grafted layer

dx.doi.org/10.1021/la301031b | Langmuir 2012, 28, 8072−8083

transforms from an open to a "supercollapsed" state—a very dense polymer layer where interchain interactions of the charged side groups occur—then the resistance to ion transport to the ECP will increase, and the grafted polymer could be approximated as a very thin dielectric layer with consequentially high capacitance.[5] For PMPDSAH, the nonassociated state becomes more stable with increasing temperature, leading to an upper critical solution temperature (UCST) for these zwitterionic polymers, both in solution[31] and as surface-grafted brushes.[2] So, at higher temperature, the supercollapsed state cannot be accessed. We presume that the nonassociated state offers no barrier to ion transport into and out of the ECP surface. Hence, at higher temperature there is no switch. In the reduced state there was little or no difference in impedance between the modified and unmodified layers. Therefore, the interpretation is that, when the ECP is in the reduced state, the grafted layer is in the nonassociated state. Thus, in the reduced and nonassociated state, the equivalent circuit parameters R_1 and q_2 are associated with charging of the conducting polymer–solution interface, controlled by the resistivity of the conducting polymer. In the oxidized and supercollapsed state, on the other hand, the equivalent circuit parameters R_1 and q_2 are associated with charging of the grafted layer and with capacitance determined by its thickness and resistance determined by its resistance to ionic movement. For the PMPDSAH surface-grafted conducting polymer, in the oxidized state, the graft is in a supercollapsed state at all salt concentrations in the range investigated, with an additional increase of density at the lower salt concentrations indicated by the increase of the charging resistance, R_1. The changes in surface wettability are consistent with these ideas. The collapsed state should be relatively hydrophobic,[2] as indeed observed for the oxidized grafted polymer, and the open state relatively hydrophilic,[2] as indeed observed for the reduced grafted polymer.

The response of the PMMA-*b*-PMPDSAH-grafted film to changes in ionic composition in solution was different to that of the PMPDSAH-grafted film. The first obvious difference is that the transition temperature for observation of the electrochemical switch was increased. The second was that the salt concentration required to develop the electrochemical switching was also increased. Following the interpretation developed for the PMPDSAH-grafted films, the variation of the equivalent circuit parameters R_1 and q_2 for the block-copolymer-grafted films implies that, when the conducting polymer was in its oxidized state, these films were in the open, nonassociated state at low salt concentration and transformed to the collapsed state when the salt concentration was increased above 0.01 M. Again, parallels can be found in the literature on the solubility and aggregation behavior of hydrophobically modified polymeric betaines. The interactions of the hydrophobic segments with each other and with the solvent significantly modify the behavior.[36] Other systems with hydrophobic-block-hydrophilic polymer structures exhibit a lower critical solution temperature (LCST), at which the polymer chains switch to a self-associated state in response to salt addition and heating.[27,71]

In solution, the dipole-associated, aggregated, or collapsed state is found in the absence of salt. Osmotic effects, counterion association with the charged sites of the zwitterion, and changes in solvation caused by salt in the solution lead to disassociation of the dipoles. For the PMPDSAH graft on the ECP surface, therefore, the reduced state would seem to correspond to the high-salt solution state and the oxidized state to the low-salt solution state, both essentially independent of the salt concentration in the electrolyte. It seems therefore a remarkable fact that, while the solution polymer is known to be essentially dissociated by rather small concentrations of NaCl, the behavior of the surface-bound PMPDSAH was dominated by the oxidation state of the conducting polymer and relatively little influenced by the salt concentration in solution.

We can develop the interpretation as follows. The conducting polymer is synthesized in the oxidized state, with the oxidized polymer charge balanced by incorporated anions. Reduction can involve either expulsion of anions or (perhaps less likely from the present literature,[68,72] though consistent with the shift to more positive potential of the cathodic reduction peak as the solution salt concentration is increased) absorption of cations to balance the charge of immobilized incorporated anions.

However, the redox process in aqueous solution does not necessarily proceed throughout the volume of the conducting polymer: indeed, the phenomenon of microstructure collapse limiting the extent of the redox process in aqueous solution is well-documented.[73] Thus, it is reasonable to suggest that charge-balancing exchangeable ions in the reduced state are located in sites close to or on the conducting polymer surface, which in the case of the films carrying grafted layers would be the interface between the conducting polymer and the surface graft. We propose that the surface-grafted layer acts as a kind of inner Helmholtz layer, storing the charge that balances the conducting polymer charge. Hence, for example, to develop the argument for the particular case of exchangeable cations, in the reduced state of the conducting polymer, exchangeable cations would adsorb to and screen the anionic sulfonate charge on the zwitterionic graft and act to expand the grafted layer, as a consequence of the intermolecular repulsion of the positive charges on the quaternary ammonium group. When these exchangeable cations were expelled upon oxidation of the conducting polymer, the grafted layer would collapse because the screening charges had been removed: the supercollapsed state promoted by strong dipolar interactions between adjacent polymer molecules on the surface. A similar argument can be developed for exchangeable anions. At higher temperatures, the thermal motion of the polymer chains negates this effect and the zwitterion charges are effectively screened by the electrolyte at all concentrations investigated in this work. The smaller values for the charging resistance, R_1, at higher salt concentration and lower temperature can be attributed to some screening by the electrolyte causing a partial expansion of the grafted layer.

The effect of the hydrophobic outer block of the PMMA-*b*-PMPDSAH-grafted film was to change the behavior: the grafted layer on the oxidized conducting polymer was in a nonassociated state at low salt concentrations but changed to a collapsed state at high salt concentration. As has previously been noted, the surface density of the grafted polymer is an important parameter whose effect we have not thus far explored. Intermolecular interactions at high surface grafting density are assumed to lead to the supercollapsed state; intramolecular interactions would lead simply to folding of the side chains. We speculate that the effect of the hydrophobic block was to weaken the intermolecular interactions and thus expand the grafted layer, to an extent dependent on the interaction of the hydrophobic block with the solvent. Salt-induced strengthening of hydrophobic interactions could

stabilize compact conformations of the hydrophobic block[74] and lessen its effect on intermolecular interactions of the zwitterionic block, leading in this case to a salt-induced collapse of the layer. These salt-induced effects are perhaps reflected in the different behavior in cyclic voltammetry of the block-copolymer-grafted films. The variations of the other parameters of the fitting, q_1 and α, reflect in different ways the charge distribution at the outer surface of the polymer film and are clearly also sensitive to the conformation of the surface-grafted layer.

5. CONCLUSIONS

We have successfully synthesized PMPDSAH- and PMMA-*b*-PMPDSAH-grafted poly(Py-*co*-PBA) films. An electrochemically controlled conformational switch of surface-modified polymer films has been achieved. This switch results from the intermolecular interaction of the grafted zwitterionic polymer brushes on a conducting polymer surface, which is sensitive to the ionic composition in the immediate vicinity of the interface. The switch is consequently dependent upon the oxidation state of the ECP, with secondary effects due to the ionic strength of the solution and the temperature. We have shown that the nature of the grafted polymer brushes can be manipulated to alter the switching behavior in aqueous solution, by grafting a block copolymer brush having a hydrophobic poly(methyl methacrylate) block outside the zwitterionic block. We have deduced that the behavior of these systems is subtly affected by salt-mediated interactions with the solvent and anticipate that the behavior could also be strongly influenced by the surface density of the polymer graft. The collapse or expansion of the graft should also be detectable by the effect on the redox reaction on the polymer surface of couples whose reversible potential lies within the range over which the switch is observable. We further anticipate that these materials will find use in the electrochemical control of surface properties, such as adhesion,[26] and will be useful in microfluidic and sensor devices.

■ ASSOCIATED CONTENT

Ⓢ Supporting Information

XPS survey spectra, table of composition data derived from XPS, and FTIR spectra. This material is available free of charge via the Internet at http://pubs.acs.org.

■ AUTHOR INFORMATION

Corresponding Author

*E-mail: david.williams@auckland.ac.nz. Telephone: (+64) 9 3737599, ext 89877.

Notes

The authors declare no competing financial interest.

■ ACKNOWLEDGMENTS

We acknowledge funding from the Ministry for Science and Innovation, New Zealand. We thank the Centre for Advanced Macromolecular Design (CAMD) group at the University of New South Wales, Australia, for advice on CRP techniques. The authors thank Dr. Colin Doyle and Dr. Michel Nieuwoudt for their help in XPS and FTIR experiments. We thank Bhuvaneswari Kannan and Ashveen Nand for scientific discussions.

■ REFERENCES

(1) Farhan, T.; Azzaroni, O.; Huck, W. T. S. AFM Study of Cationically Charged Polymer Brushes: Switching between Soft and Hard Matter. *Soft Matter* **2005**, *1*, 66−68.
(2) Azzaroni, O.; Brown, A. A.; Huck, W. T. S. UCST Wetting Transitions of Polyzwitterionic Brushes Driven by Self-Association. *Angew. Chem., Int. Ed.* **2006**, *45*, 1770−1774.
(3) Azzaroni, O.; Trappmann, B.; van Rijn, P.; Zhou, F.; Kong, B.; Huck, W. T. S. Mechanically Induced Generation of Counterions Inside Surface-Grafted Charged Macromolecular Films: Towards Enhanced Mechanotransduction in Artificial Systems. *Angew. Chem., Int. Ed.* **2006**, *45*, 7440−7443.
(4) Zhou, F.; Huck, W. T. S. Surface Grafted Polymer Brushes as Ideal Building Blocks for "Smart" Surfaces. *Phys. Chem. Chem. Phys.* **2006**, *8*, 3815−3823.
(5) Zhou, F.; Hu, H. Y.; Yu, B.; Osborne, V. L.; Huck, W. T. S.; Liu, W. M. Probing the Responsive Behavior of Polyelectrolyte Brushes Using Electrochemical Impedance Spectroscopy. *Anal. Chem.* **2007**, *79*, 176−182.
(6) Choi, E. Y.; Azzaroni, O.; Cheng, N.; Zhou, F.; Kelby, T.; Huck, W. T. S. Electrochemical Characteristics of Polyelectrolyte Brushes with Electroactive Counterions. *Langmuir* **2007**, *23*, 10389−10394.
(7) Azzaroni, O.; Brown, A. A.; Huck, W. T. S. Tunable Wettability by Clicking Counterions Into Polyelectrolyte Brushes. *Adv. Mater.* **2007**, *19*, 151−154.
(8) Yu, B.; Hu, H. Y.; Wang, D. A.; Huck, W. T. S.; Zhou, F.; Liu, W. M. Electrolyte-Modulated Electrochemistry and Electrocatalysis on Ferrocene-Terminated Polyelectrolyte Brushes. *J. Mater. Chem.* **2009**, *19*, 8129−8134.
(9) Zhou, F.; Biesheuvel, P. M.; Choi, E.-Y.; Shu, W.; Poetes, R.; Steiner, U.; Huck, W. T. S. Polyelectrolyte Brush Amplified Electroactuation of Microcantilevers. *Nano Lett.* **2008**, *8*, 725−730.
(10) Skotheim, T. A.; Reynolds, J. R. *Handbook of Conducting Polymers*, 3rd ed.; CRC: London, 1986.
(11) Andersson, M.; Ekeblad, P. O.; Hjertberg, T.; Wennerstrom, O.; Inganas, O. Polythiophene with a Free Amino-Acid Side-Chain. *Polym. Commun.* **1991**, *32*, 546−548.
(12) Teh, K. S.; Takahashi, Y.; Yao, Z.; Lu, Y.-W. Influence of Redox-Induced Restructuring of Polypyrrole on Its Surface Morphology and Wettability. *Sens. Actuators A: Phys.* **2009**, *155*, 113−119.
(13) Heinze, J.; Frontana-Uribe, B. A.; Ludwigs, S. Electrochemistry of Conducting Polymers—Persistent Models and New Concepts. *Chem. Rev.* **2010**, *110*, 4724−4771.
(14) Isaksson, J.; Tengstedt, C.; Fahlman, M.; Robinson, N.; Berggren, M. A Solid-State Organic Electronic Wettability Switch. *Adv. Mater.* **2004**, *16*, 316−320.
(15) Chang, J. H.; Hunter, L. W. A Superhydrophobic to Superhydrophilic In Situ Wettability Switch of Microstructured Polypyrrole Surfaces. *Macromol. Rapid Commun.* **2011**, *32*, 718−723.
(16) Xin, B.; Hao, J. Reversibly Switchable Wettability. *Chem. Soc. Rev.* **2010**, *39*, 769−782.
(17) Tsai, Y.-T.; Choi, C.-H.; Gao, N.; Yang, E.-H. Tunable Wetting Mechanism of Polypyrrole Surfaces and Low-Voltage Droplet Manipulation via Redox. *Langmuir* **2011**, *27*, 4249−4256.
(18) Xu, L.; Chen, W.; Mulchandani, A.; Yan, Y. Reversible Conversion of Conducting Polymer Films from Superhydrophobic to Superhydrophilic. *Angew. Chem., Int. Ed.* **2005**, *44*, 6009−6012.
(19) Robinson, L.; Isaksson, J.; Robinson, N. D.; Berggren, M. Electrochemical Control of Surface Wettability of Poly(3-alkylthiophenes). *Surf. Sci.* **2006**, *600*, L148−L152.
(20) Xu, L.; Wang, J.; Song, Y.; Jiang, L. Electrically Tunable Polypyrrole Inverse Opals with Switchable Stopband, Conductivity, and Wettability. *Chem. Mater.* **2008**, *20*, 3554−3556.
(21) Aulich, D.; Hoy, O.; Luzinov, I.; Eichhorn, K.-J.; Stamm, M.; Gensch, M.; Schade, U.; Esser, N.; Hinrichs, K. In-Situ IR Synchrotron Mapping Ellipsometry on Stimuli-Responsive PAA-*b*-PS/PEG Mixed Polymer Brushes. *Phys. Status Solidi C* **2010**, *7*, 197−199.

(22) Jones, D. M.; Brown, A. A.; Huck, W. T. S. Surface-Initiated Polymerizations in Aqueous Media: Effect of Initiator Density. *Langmuir* **2002**, *18*, 1265−1269.
(23) Coessens, V.; Pintauer, T.; Matyjazewski, K. Functional Polymers by Atom Transfer Radical Polymerziation. *Prog. Polym. Sci.* **2001**, *26*, 337−377.
(24) Zhao, B.; Brittain, W. J. Polymer Brushes: Surface-Immobilized Macromolecules. *Prog. Polym. Sci.* **2000**, *25*, 677−710.
(25) Roux, S.; Duwez, A.-S.; Demoustier-Champagne, S. Surface Initiated Polymerization of Styrene from a Carboxylic Acid Functionalized Polypyrrole Coated Electrode. *Langmuir* **2003**, *19*, 306−313.
(26) Strover, L.; Roux, C.; Malmström, J.; Pei, Y.; Williams, D. E.; Travas-Sejdic, J. Switchable Surfaces of Electroactive Polymer Brushes Grafted from Polythiophene ATRP-Macroinitiator. *Synth. Met.* **2012**, *162*, 381−390.
(27) Virtanen, J.; Arotcuarena, M.; Heise, B.; Ishaya, S.; Laschewsky, A.; Tenhu, H. Dissolution and Aggregation of a Poly(NIPA-*block*-sulfobetaine) Copolymer in Water and Saline Aqueous Solutions. *Langmuir* **2002**, *18*, 5360−5365.
(28) Hart, R.; Timmerman, D. New Polyampholytes: The Polysulfobetaines. *J. Polym. Sci.* **1958**, *28*, 638−640.
(29) Soto, V. M. M.; Galin, J. C. Poly(sulphopropylbetaines): 2. Dilute Solution Properties. *Polymer* **1984**, *25*, 254−262.
(30) Lowe, A. B.; McCormick, C. L. Synthesis and Solution Properties of Zwitterionic Polymers. *Chem. Rev.* **2002**, *102*, 4177−4189.
(31) Mary, P.; Bendejacq, D. D.; Labeau, M. P.; Dupuis, P. Reconciling Low- and High-Salt Solution Behavior of Sulfobetaine Polyzwitterions. *J. Phys. Chem. B* **2007**, *111*, 7767−7777.
(32) Georgiev, G. S.; Karnenska, E. B.; Vassileva, E. D.; Kamenova, I. P.; Georgieva, V. T.; Iliev, S. B.; Ivanov, I. A. Self-Assembly, Antipolyelectrolyte Effect, and Nonbiofouling Properties of Polyzwitterions. *Biomacromolecules* **2006**, *7*, 1329−1334.
(33) Kumar, R.; Fredrickson, G. H. Theory of Polyzwitterion Conformations. *J. Chem. Phys.* **2009**, *131*, 104901−16.
(34) Che, Y. J.; Tan, Y. B.; Cao, J.; Xin, H. P.; Xu, G. Y. Synthesis and Properties of Hydrophobically Modified Acrylamide-Based Polysulfobetaines. *Polym. Bull.* **2011**, *66*, 17−35.
(35) Johnson, K. M.; Fevola, M. J.; McCormick, C. L. Hydrophobically Modified Acrylamide-Based Polybetaines. I. Synthesis, Characterization, and Stimuli-Responsive Solution Behavior. *J. Appl. Polym. Sci.* **2004**, *92*, 647−657.
(36) Che, Y. J.; Tan, Y. B.; Cao, J.; Xu, G. Y. A Study of Aggregation Behavior of a Sulfobetaine Copolymer in Dilute Solution. *J. Polym. Res.* **2010**, *17*, 557−566.
(37) Chen, M.; Briscoe, W. H.; Armes, S. P.; Klein, J. Lubrication at Physiological Pressures by Polyzwitterionic Brushes. *Science* **2009**, *323*, 1698−1701.
(38) Kong, B.; Choi, J. S.; Jeon, S.; Choi, I. S. The Control of Cell Adhesion and Detachment on Thin Films of Thermoresponsive Poly[(*N*-isopropylacrylamide)-r-((3-(methacryloylamino)propyl)-dimethyl(3-sulfopropyl)ammonium hydroxide)]. *Biomaterials* **2009**, *30*, 5514−5522.
(39) Cheng, G.; Li, G.; Xue, H.; Chen, S.; Bryers, J. D.; Jiang, S. Zwitterionic Carboxybetaine Polymer Surfaces and Their Resistance to Long-Term Biofilm Formation. *Biomaterials* **2009**, *30*, 5234−5240.
(40) Dai, F.; Wang, P.; Wang, Y.; Tang, L.; Yang, J.; Liu, W.; Li, H.; Wang, G. Double Thermoresponsive Polybetaine-Based ABA Triblock Copolymers with Capability to Condense DNA. *Polymer* **2008**, *49*, 5322−5328.
(41) Cho, W. K.; Kong, B.; Choi, I. S. Highly Efficient Non-Biofouling Coating of Zwitterionic Polymers: Poly((3-(methacryloylamino)propyl)-dimethyl(3-sulfopropyl)ammonium hydroxide). *Langmuir* **2007**, *23*, 5678−5682.
(42) Su, Y.; Zheng, L.; Li, C.; Jiang, Z. Smart Zwitterionic Membranes with On/Off Behavior for Protein Transport. *J. Phys. Chem. B* **2008**, *112*, 11923−11928.
(43) Jiang, W.; Awasum, J. N.; Irgum, K. Control of Electroosmotic Flow and Wall Interactions in Capillary Electrophoresis Capillaries by Photografted Zwitterionic Polymer Surface Layers. *Anal. Chem.* **2003**, *75*, 2768−2774.
(44) Keefe, A. J.; Jiang, S. Poly(zwitterionic)protein Conjugates Offer Increased Stability Without Sacrificing Binding Affinity or Bioactivity. *Nat. Chem.* **2012**, *4*, 59−63.
(45) Polzer, F.; Heigl, J.; Schneider, C.; Ballauff, M.; Borisov, O. V. Synthesis and Analysis of Zwitterionic Spherical Polyelectrolyte Brushes in Aqueous Solution. *Macromolecules* **2011**, *44*, 1654−1660.
(46) Kikuchi, M.; Terayama, Y.; Ishikawa, T.; Hoshino, T.; Kobayashi, M.; Ogawa, H.; Masunaga, H.; Koike, J.-i.; Horigome, M.; Ishihara, K.; Takahara, A. Chain Dimension of Polyampholytes in Solution and Immobilized Brush States. *Polym. J.* **2012**, *44*, 121−130.
(47) Lassalle, N.; Vieil, E.; Correia, J. P.; Abrantes, L. M. Study of DNA Hybridization on Polypyrrole Grafted with Oligonucleotides by Photocurrent Spectroscopy. *Biosens. Bioelectron.* **2011**, *16*, 295−303.
(48) Vigmond, S. J.; Kallury, K. M. R.; Thompson, M. Pyrrole Copolymerization and Polymer Derivatization Studied by X-ray Photoelectron Spectroscopy. *Anal. Chem.* **1992**, *64*, 2763−2769.
(49) Bisquert, J.; Garcia-Belmonte, G.; Fabregat-Santiago, F.; Compte, A. Anomalous Transport Effects in the Impedance of Porous Film Electrodes. *Electrochem. Commun.* **1999**, *1*, 429−435.
(50) Garcia-Belmonte, G.; Bisquert, J. Impedance Analysis of Galvanostatically Synthesized Polypyrrole Films. Correlation of Ionic Diffusion and Capacitance Parameters with the Electrode Morphology. *Electrochim. Acta* **2002**, *47*, 4263−4272.
(51) Garcia-Belmonte, G.; Fabregat-Santiago, F.; Bisquert, J.; Yamashita, M.; Pereira, E. C.; Castro-Garcia, S. Frequency Dispersion in Electrochromic Devices and Conducting Polymer Electrodes: A Generalized Transmission Line Approach. *Ionics* **1999**, *5*, 44−51.
(52) Bisquert, J.; Belmonte, G. G.; Santiago, F. F.; Ferriols, N. S.; Yamashita, M.; Pereira, E. C. Application of a Distributed Impedance Model in the Analysis of Conducting Polymer Films. *Electrochem. Commun.* **2000**, *2*, 601−605.
(53) Moreira, L.; Martins, F. Design of an Excel Spreadsheet To Estimate Rate Constants, Determine Associated Errors, and Choose Curve's Extent. *J. Chem. Educ.* **2006**, *83*, 1879−1883.
(54) Feller, S. E.; Blaich, C. F. Error Estimates for Fitted Parameters: Application to HCl/DCl Vibrational−Rotational Spectroscopy. *J. Chem. Educ.* **2001**, *78*, 409−412.
(55) de Levie, R. Estimating Parameter Precision in Nonlinear Least Squares with Excel's Solver. *J. Chem. Educ.* **1999**, *76*, 1594−1598.
(56) de Levie, R. *Advanced Excel for Scientific Data Analysis*; Oxford University Press: Oxford, 2008.
(57) Batz, P.; Schmeisser, D.; Gopel, W. Electronic Structure of Polypyrrole Films. *Phys. Rev. B* **1991**, *43*, 9178−9189.
(58) Rosso, F.; Barbarisi, A.; Barbarisi, M.; Petillo, O.; Margarucci, S.; Calarco, A.; Peluso, G. New Polyelectrolyte Hydrogels for Biomedical Applications. *Mater. Sci. Eng. C* **2003**, *23*, 371−376.
(59) Madani, A.; Nessark, B.; Brayner, R.; Elaissari, H.; Jouini, M.; Mangeney, C.; Chehimi, M. M. Carboxylic Acid-Functionalized, Core-Shell Polystyrene@Polypyrrole Microspheres as Platforms for the Attachment of CdS Nanoparticles. *Polymer* **2010**, *51*, 2825−2835.
(60) Pfluger, P.; Street, G. B. Chemical, Electronic, and Structural Properties of Conducting Heterocyclic Polymers: A View by XPS. *J. Chem. Phys.* **1984**, *80*, 544−553.
(61) Stach, M.; Kroneková, Z.; Kasák, P.; Kollár, J.; Pentrák, M.; Mičušík, M.; Chorvat, D.; Nunney, T. S.; Lacík, I. Polysulfobetaine Films Prepared by Electrografting Technique for Reduction of Biofouling on Electroconductive Surfaces. *Appl. Surf. Sci.* **2011**, *257*, 10795−10801.
(62) Kaczmarek, H.; Chaberska, H. AFM and XPS Study of UV-Irradiated Poly(methyl methacrylate) Films on Glass and Aluminum Support. *Appl. Surf. Sci.* **2009**, *255*, 6729−6735.
(63) Ton-That, C.; Shard, A. G.; Teare, D. O. H.; Bradley, R. H. XPS and AFM Surface Studies of Solvent-Cast PS/PMMA Blends. *Polymer* **2001**, *42*, 1121−1129.
(64) Brinkhuis, R. H. G.; Schouten, A. J. Thin-Film Behavior of Poly(methyl methacrylates). 2. An FT-IR Study of Langmuir-Blodgett Films of Isotactic PMMA. *Macromolecules* **1991**, *24*, 1496−1504.

(65) van der Sluijs, M. J.; Underhill, A. E.; Zaba, B. N. Electrochemistry of Polypyrrole Films. *J. Phys. D: Appl. Phys.* **1987**, *20*, 1411−1416.
(66) Diaz, A. F.; Castillo, J. I.; Logan, J. A.; Lee, W.-Y. Electrochemistry of Conducting Polypyrrole Films. *J. Electroanal. Chem. Interfacial Electrochem.* **1981**, *129*, 115−132.
(67) Li, S.; Qiu, Y.; Guo, X. Influence of Doping Anions on the Ion Exchange Behavior of Polypyrrole. *J. Appl. Polym. Sci.* **2009**, *114*, 2307−2314.
(68) Inzelt, G.; Kertész, V.; Nybäck, A.-S. Electrochemical Quartz Crystal Microbalance Study of Ion Transport Accompanying Charging-Discharging of Poly(pyrrole) Films. *J. Solid State Electrochem.* **1999**, *3*, 251−257.
(69) Gabrielli, C.; Perrot, H.; Rubin, A.; Pham, M. C.; Piro, B. Ac-Electrogravimetry Study of Ionic Exchanges on a Polypyrrole Modified Electrode in Various Electrolytes. *Electrochem. Commun.* **2007**, *9*, 2196−2201.
(70) Levi, M. D.; Lopez, C.; Vieil, E.; Vorotyntsev, M. A. Influence of Ionic Size on the Mechanism of Electrochemical Doping of Polypyrrole Films Studied by Cyclic Voltammetry. *Electrochim. Acta* **1997**, *42*, 757−769.
(71) Nedelcheva, A. N.; Novakov, C. P.; Miloshev, S. M.; Berlinova, I. V. Electrostatic Self-Assembly of Thermally Responsive Zwitterionic Poly(N-isopropylacrylamide) and Poly(ethylene oxide) Modified with Ionic Groups. *Polymer* **2005**, *46*, 2059−2067.
(72) Aulich, D.; Hoy, O.; Luzinov, I.; Brucher, M.; Hergenroder, R.; Bittrich, E.; Eichhorn, K. J.; Uhlmann, P.; Stamm, M.; Esser, N.; Hinrichs, K. In Situ Studies on the Switching Behavior of Ultrathin Poly(acrylic acid) Polyelectrolyte Brushes in Different Aqueous Environments. *Langmuir* **2010**, *26*, 12926−12932.
(73) Spires, J. B.; Peng, H.; Williams, D. E.; Soeller, C.; Travas-Sejdic, J. Solvent-Induced Microstructure Changes and Consequences for Electrochemical Activity of Redox-Active Conducting Polymers. *Electrochim. Acta* **2010**, *55*, 3061−3067.
(74) Ghosh, T.; Kalra, A.; Garde, S. On the Salt-Induced Stabilization of Pair and Many-Body Hydrophobic Interactions. *J. Phys. Chem. B* **2005**, *109*, 642−651.